



McGookin, M. and Anderson, D. and McGookin, E. (2008) *Application of MPC and sliding mode control to IFAC benchmark models*. In: UKACC International Conference on Control 2008, 2-4 Sept 2008, Manchester, UK.

<http://eprints.gla.ac.uk/5040/>

Deposited on: 7 July 2009

Application of MPC and Sliding Mode Control To IFAC Benchmark Models

Meghan McGookin*. David Anderson**
Euan William McGookin***

*Department of Aerospace Engineering, University of Glasgow, Glasgow, U.K. (Tel: +44 (0) 141 330 3575; e-mail: m.mcgookin@eng.gla.ac.uk)

** Department of Aerospace Engineering, University of Glasgow, Glasgow, U.K. (e-mail: d.anderson@aero.gla.ac.uk u)

*** Department of Aerospace Engineering, University of Glasgow, Glasgow, U.K.
(e-mail: e.mcgookin@eng.gla.ac.uk)

Abstract: The comparison of Model Predictive Control (MPC) and Sliding Mode Control (SMC) are presented in this paper. This paper investigates the performance of each controller as the navigation system for IFAC benchmark ship models (cargo vessel and oil tanker). In this investigation the navigation system regulates the heading angle of the two types of marine vessel with reference to a desired heading trajectory. In this investigation, the result obtained from MPC is compared with a well-established control methodology, namely Sliding Mode control theory. Wave disturbances and actuator limits are implemented to provide a more realistic evaluation and comparison for the proposed control structure.

1. INTRODUCTION

Navigation safety has become a major issue for marine vessel operators in the last few decades. This is mainly due to the increase in size and number of cargo vessels and super tankers that operate in the world's oceans. Unpredictable errors occurring in the navigation control and practices of these huge vessels have resulted in accidents and associated oil spills for oil tanker vessel. The occurrence of such faults has come at a cost, in terms of associated environmental damage and clean-up operations (Loo, 2005). Hence, it is important that such accidents can be reduced (McGookin *et al.*, 2000). However, such improvements are not easily achieved due to the limited operational range of the rudder, which is the primary actuator for ship steering control in vessels of this kind. In order to provide a rapid and large change in the ship's heading trajectory, a large rudder deflection is usually required to provide such manoeuvres (Fossen, 1994) and such deflections may take the rudder to its saturation limits. In such circumstances there is no control authority to deal with further unexpected navigational demands or to compensate for external disturbances, such as waves, resulting in the vessel becoming temporarily uncontrollable (McGookin *et al.*, 2000).

Considerable research has been carried out in the development of navigation systems that reduce the risk of extreme scenarios of the type outlined above (Källström *et al.*, 1979; Fossen, 1994; McGookin *et al.*, 2000). In this paper, an advanced optimal control methodology, namely, *Model Predictive Control* (MPC) is investigated. The main advantage of implementing MPC is its ability to 'predict' the current input based on the future trajectory. The performance of MPC is compared with another control theory, namely, Sliding Mode (SM) control.

The IFAC benchmark models, which consist of linearised mathematical models of a cargo ship and an oil tanker, have been used to evaluate the performance of MPC and SM controllers (Maciejowski, 2002; McGookin *et al.* 2000). Wave disturbances are implemented within the system simulation to investigate the disturbance rejection capabilities of these two control theories (Fossen, 1994).

2. SIMULATION MODEL

The simulation models consist of the dynamics and kinematics of the vehicles, and the external induced forces generated by waves. These are discussed in the sections below.

2.1. Linearised Vessel Models

Two linearised models representing the heading dynamics of cargo vessel (161m long) and an oil tanker (322m long) are used as the control subjects for this study. These are defined as IFAC benchmark models (Källström *et al.*, 1979). Both vessels are travelling at a constant forward speed (refer to Appendix A for speed values). The IFAC benchmark models is represented by standard state-space form, i.e:

$$\dot{\mathbf{x}} = \mathbf{A}\mathbf{x} + \mathbf{B}\mathbf{u} \quad (1)$$

Here \mathbf{x} is the system states vector, \mathbf{u} is the control input vector, \mathbf{A} is the system matrix and, \mathbf{B} is the input matrix. The data of both vessels are shown in Appendix A. The heading autopilot is designed based on the decoupled dynamics of \mathbf{x} and are represented in terms of v (sway velocity), r (yaw rate) and ψ (heading angle), and usually provide a basis to design heading autopilots. The input for this study is the rudder angle, δr (deg) as shown in Fig 1.

Even though the vessels used throughout this investigation are linearised models, the nonlinear dynamics of the rudder actuator are incorporated in the form of maximum rudder deflection ($\pm 40^\circ$) and the rate of rudder motion ($\pm 10^\circ/\text{sec}$).

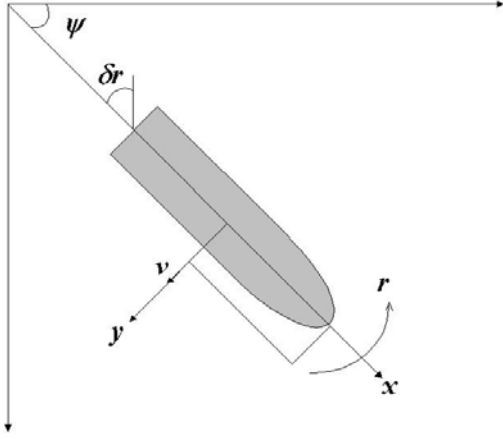


Fig 1. Notation Used to Describe Ship's Motion

As a result, both the vessels and their associated controllers that operate within these limits, the response, ψ must not exhibit any overshoots. To satisfy this design specification, the desired response of the heading angle, ψ , is designed to be a zig-zag critically damped second order response (Källström *et al.*, 1979; Fossen, 1994).

2.2. Wave Disturbances

System robustness to the effects of environmental disturbances can be investigated using wave disturbances within the computer-based model of the vessel and the associated controller. Wind generated waves are considered as it is to be the most relevant disturbance for surface vessels, it represents wave spectra of a fully developed sea of the North Atlantic Ocean (Fossen, 1994). The PM spectrum is written as:

$$S(\omega) = 0.0081 g^2 \omega^{-5} \exp(-3.11 \omega^{-4} / H_s^2) \quad (3)$$

Here H_s is the significant wave height (m). In this application, the significant wave height of 3m for cargo vessel and 5m for tanker vehicle are chosen, which corresponds to very rough sea conditions.

3. CONTROL METHODOLOGIES

This paper describes an approach to guidance/navigation system design that involves two advanced control methodologies, namely *Sliding Mode* (SM) control and *Model Predictive Control* (MPC).

3.1. Sliding Mode Control Theory

The first control methodologies investigated in this paper is *Sliding Mode* (SM) control theory, which is used to design the feedback navigation system. (Edwards and Spurgeon, 1998; McGookin *et al.* 2000). The advantage of using SM control in this application is that it can provide inherent robustness to compensate for uncertainties caused by unmodelled dynamics and/or external disturbances (McGookin *et al.*, 2000).

with the associated forces and moments induced by a regular sea on a block-shaped ship (Fossen, 1994) The resulting forces act in the direction of the X , Y forces and the N moment are X_{wave} , Y_{wave} , and N_{wave} respectively. These wave force components form a vector called τ_w , and by applying the principle of linear superposition (Fossen, 1994), the wave forces and moments are added to the state-space equation shown in Equation (1), $\dot{x} = f(x, u, \tau_w)$. The vector, τ_w , consists of three components, namely:

$$\tau_w = \begin{bmatrix} \sum_{i=1}^N \rho g B L T \cos(\beta - \psi) [A_i k_i \sin(\omega_{ei} + \phi_i)] \\ \sum_{i=1}^N -\rho g B L T \sin(\beta - \psi) [A_i k_i \sin(\omega_{ei} + \phi_i)] \\ \sum_{i=1}^N \frac{1}{24} \rho g B L (L^2 - B^2) \sin 2(\beta - \psi) [A_i k_i \sin(\omega_{ei} + \phi_i)] \end{bmatrix} \quad (2)$$

Here B , L and T are the breadth (m), length (m) and draft (m) respectively, of the wetted part of the vessel, represented as a rectangular cuboid. The term ρ is the density of water (kg/m^3), g is the acceleration due to gravity (m/s^2) and $(\beta - \psi)$ is the angle between the heading of the ship and the direction of the wave (rad). In addition, ω_{ei} is the frequency of encounter corresponding to wave component, i and ϕ_i is a random phase angle, uniformly distributed. A_i is the wave amplitude, ($A_i^2 = 2S(\omega_i)\Delta\omega$) and k_i is the wave number, ($k_i = \omega_i^2/g$) with ω_i is the wave frequency of wave component, and $\Delta\omega$ is a constant difference between successive frequencies.

In this paper, the Pierson-Moskowitz (PM) Wave Spectrum is chosen as

In this application, the design of the SM controller is based a SISO linear representation of the heading dynamics for the models (Healey and Marco, 1992). This controller regulates the heading angle (ψ) of the vessel by providing the required rudder deflection, δr_c signal. The SM control action regulates the measurement error between the desired and actual states. Using this information, the SM controller generates the required control action for accurate tracking. The SM control methodology used here is based on a SISO state-space representation of the dynamics of the vessels, similar to Equation (1).

All the control action provided by SM controller is through the single input, u_{FB} , of the system. By definition (Edwards and Spurgeon, 1998; McGookin *et al.*, 2000), such control action of SM control has two distinct elements:

$$u_{FB} = u_{eq} + u_{sw} \quad (6)$$

where u_{eq} is called the equivalent control signal and u_{sw} is called the switching control signal.

The nominal equivalent control component is chosen as a state feedback gain controller, which is based on a linearised controller. It can be represented by:

$$u_{eq} = -\mathbf{K}^T \mathbf{x} \quad (7)$$

Here \mathbf{K}^T is the transpose of the feedback gain matrix, \mathbf{K} . This is achieved through robust EA. The additional control is provided by the nonlinear switching term is derived from a

state hyperplane called the *sliding surface*, σ (Healey and Marco, 1992; Fossen, 1994; McGookin *et al.*, 2000) and can be represented by the following equation:

$$\sigma(\Delta \mathbf{x}) = \mathbf{h}^T \Delta \mathbf{x} = \mathbf{h}^T (\mathbf{x}_d - \mathbf{x}) \quad (8)$$

This is a function of the state error $\Delta \mathbf{x}$ and a gain vector \mathbf{h} . Following the derivation given by McGookin, *et al.* (2000), the switching component can be represented by:

$$u_{sw} = (\mathbf{h}^T \mathbf{B})^{-1} [\mathbf{h}^T \dot{\mathbf{x}}_d - \eta \operatorname{sgn}(\dot{\sigma}(\Delta \mathbf{x}))] \quad (9)$$

The switching term provides the nonlinear action essential for SM control and, as shown in Equation (9), this is conventionally based on the discontinuous *signum* function with η as the *switching gain* (Edwards and Spurgeon, 1998; McGookin *et al.*, 2000). In the paper by Healey and Marco (1992), this hard switching is replaced by soft switching, i.e. a continuous hyperbolic tangent function. The *tanh* function has the same end points as the *signum* function (i.e., ± 1 as $\sigma \rightarrow \infty$) but the boundary layer σ has a gradual transition towards zero and the boundary layer thickness, ϕ , determines the slope of the transition (Healey and Marco, 1992). When ϕ is small the transition from -1 to 1 is fast, but as ϕ increases the transition becomes less rapid. The switching control action with the hyperbolic tangent term included can be written as:

$$u_{sw} = (\mathbf{h}^T \mathbf{B})^{-1} [\mathbf{h}^T \dot{\mathbf{x}}_d - \eta \tanh(\sigma(\Delta \mathbf{x})/\phi)] \quad (10)$$

The introduction of the boundary layer reduces the risk of chattering, which is a feature of conventional forms of SM involving the *signum* function. By combining Equation (5) and (8), the full SM control structure can be represented by:

$$u_{FB} = -\mathbf{k}^T \mathbf{x} + (\mathbf{h}^T \mathbf{B})^{-1} [\mathbf{h}^T \dot{\mathbf{x}}_d - \eta \tanh(\sigma(\Delta \mathbf{x})/\phi)] \quad (11)$$

In this application, SM controller is tuned to provide an acceptable rudder operational range but with an accurate tracking performance (Loo *et al.*, 2004).

3.2. Model Predictive Controller

The second control methodology that is investigated in this paper is the Model Predictive Control (MPC). MPC is an optimization-based closed-loop control strategy in which pointwise-in-time design constraints on system's state, input and output can be explicitly embedded into the controller and at the same time it is a closed-loop strategy, since at each time instant the optimization is repeated using the most recent measurements (Maciejowski, 2002). The first control input in the solution is applied to the system, and with the new initial conditions, an optimization is repeated on the new horizon, shifted one step ahead. Such shifting in horizon also gives the MPC an alternative term, namely 'receding horizon control'.

In this paper, a linear and discrete-time state space model can be represented by rearranging equation (1) to give:

$$\begin{aligned} \mathbf{x}(t+1) &= \mathbf{A}\mathbf{x}(t) + \mathbf{B}u(t) \\ \mathbf{y}(k) &= \mathbf{C}\mathbf{x}(t) \end{aligned} \quad (12)$$

The MPC solves the following optimisation problem for the current $\mathbf{x}(t)$ at each time t (Bemporad *et al.*, 2002):

$\min_{U, s} \{J(U, \mathbf{x}(t))\}$ subject to:

$$y_{\min} \leq y_{t+k|t} \leq y_{\max}, k=1, \dots, N$$

$$u_{\min} \leq u_{t+k} \leq u_{\max}, k=1, \dots, M-1$$

$$u_{t+k} = \mathbf{K}\mathbf{x}_{t+k|t}, M \leq k \leq N-1$$

$$\mathbf{x}_{t|t} = \mathbf{x}(t)$$

$$\mathbf{x}_{t+k+1|t} = \mathbf{A}\mathbf{x}_{t+k|t} + \mathbf{B}u_{t+k}, k \geq 0$$

$$\mathbf{y}_{t+k|t} = \mathbf{C}\mathbf{x}_{t+k|t}, k \geq 0$$

where the cost function to be minimised is given as

$$\begin{aligned} J &= \mathbf{x}_{t+N|t}^T \mathbf{P} \mathbf{x}_{t+N|t} \\ &+ \sum_{k=0}^{N-1} \{ \mathbf{x}_{t+k|t}^T \mathbf{Q} \mathbf{x}_{t+k|t} + u_{t+k}^T \mathbf{R} u_{t+k} \} \end{aligned} \quad (14)$$

and $U = [u_t^T, \dots, u_{t+M-1}^T]^T$ and $s = [s_t^T, \dots, s_{t+N-1}^T]^T$, $\mathbf{R} = \mathbf{R}^T > 0$, $\mathbf{Q} = \mathbf{Q}^T \geq 0$, $\mathbf{P} = \mathbf{P}^T$, $\mathbf{x}_{t+k|t}$ denotes the predicted state vector of $\mathbf{x}(t+k)$ at time t , obtained by applying the input sequence u_t, \dots, u_{t+k+1} to model (12) starting from the state $\mathbf{x}(t)$. M and N are input and constraint horizons. The final cost matrix \mathbf{P} and gain matrix \mathbf{K} are calculated from the algebraic Riccati equation, under the assumptions that the constraints are not active for $k \geq M$ and $k \geq N$. In addition, equation (13) solves the constrained infinite horizon LQR problem for equation (1), with weight matrices \mathbf{R} and \mathbf{Q} . For this application, the system dynamics and design constraints are linear, optimisation problem shown in (14) involves only continuous variables, and the MPC algorithm requires the solution of a Quadratic Program (QP) at each time step t .

4. SIMULATION RESULTS WITHOUT WAVE DISTURBANCES

The results presented in this section are simulation results obtained without the presence of waves.

For the IFAC benchmark models, a zig-zag manoeuvre ($\pm 45^\circ$) is chosen as the desired heading or yaw angle trajectory. A smooth 45° is relatively demanding for a large vessel such as an oil tanker or a cargo vessel. Once the ship has reached its 45° heading, it is required to change its heading from 45° to -45° , as a result, a total of 90° change in heading angle is required. In order to provide such a drastic change in yaw angle, the ship will have to drive or deflect its actuator, i.e. the rudder to almost its maximum in order to accommodate a 90° change in heading angle. Consequently, an effective and reliable controller has to be designed to provide precise heading tracking and yet, capable to utilise the rudder more effectively.

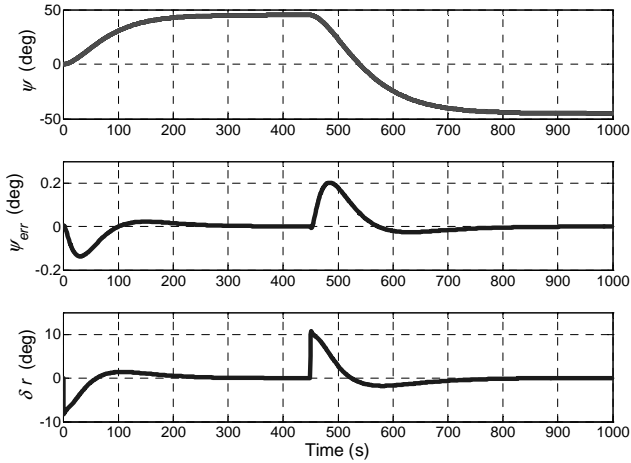


Fig 2. Cargo vessel with SM

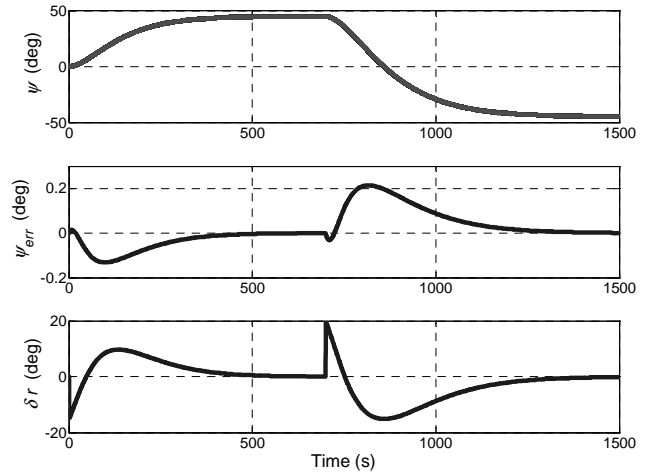


Fig 4. Oil Tanker with SM

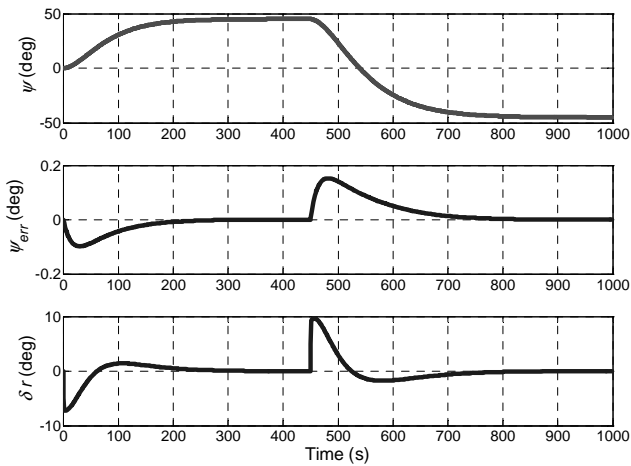


Fig 3. Cargo vessel with MPC

For the application of cargo vessel, it can be seen both feedback controller (SM in Fig 2 and MPC in Fig 3) provides excellent tracking ability with a heading error of $\pm 0.15^\circ$ and $\pm 0.2^\circ$ for SM and MPC respectively. However, on close inspection of the rudder deflection, δr , at the peak values of time at 0s and 450s (both peaks are caused by the sudden change of heading angle), the rudder performance for the MPC is slightly ‘smoother’ (gentler steer of the rudder). In addition, the rudder deflection for MPC is within the range of $\pm 10^\circ$ compared to $\pm 11^\circ$ for the SM controller.

It should be noted that SM has a nonlinear structure that has a characteristic continuous switching action. This switching action provides an inherent robustness in the form of additional control effort that compensates for unmodelled dynamics in the system. For this paper, the main objective is to provide accurate heading tracking, hence minimising the heading error. As a result, a trade-off between accurate heading tracking and minimum rudder usage exists.

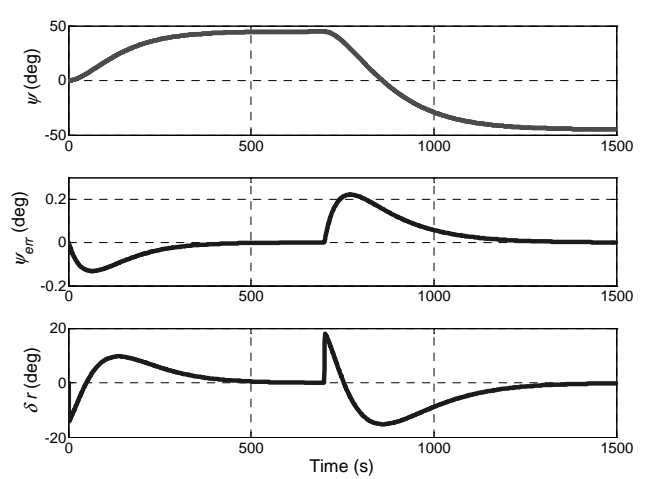


Fig 5. Oil Tanker with MPC

In the case of the oil tanker (SM in Fig 4 and MPC in Fig 5), it can be noticed that both control methodologies deliver an extremely accurate heading tracking with an error of $\pm 0.22^\circ$. Similarly, on closer inspection on the rudder deflection responses, it can be observed that MPC is able to deliver equally precise heading tracking by using marginally lesser rudder manoeuvre. This is because MPC has the ability to ‘predict’ the required rudder deflection ahead of time since the heading trajectory has been predefined. As a result, MPC generates a control action that commands the steering slightly earlier, thus producing a smoother transient response for the rudder deflection.

It can also be noticed that as the size of the vessel increases (refer to Appendix A), a larger rudder deflection is required to steer the ship towards the desired heading angle and a longer simulation time is required as well. In all cases, without the presence of wave disturbances, the heading error is less than $\pm 0.3^\circ$, which is relatively very small for a zig-zag manoeuvre of $\pm 45^\circ$ and a rudder deflection of $\pm 20^\circ$ (for $\delta r_{max} = \pm 40^\circ$) is well within its operational limits for the rudder actuator.

5. SIMULATION RESULTS WITH WAVE DISTURBANCES

The results presented in this section are simulation results obtained with the presence of waves. The significant wave height chosen to conduct the controller tracking ability corresponds to a rough sea description (significant wave height of $H_s = 3\text{m}$ for cargo and $H_s = 5\text{m}$ for oil tanker vessel) and thus the rudder has to respond rapidly in order to achieve the manoeuvring trajectory.

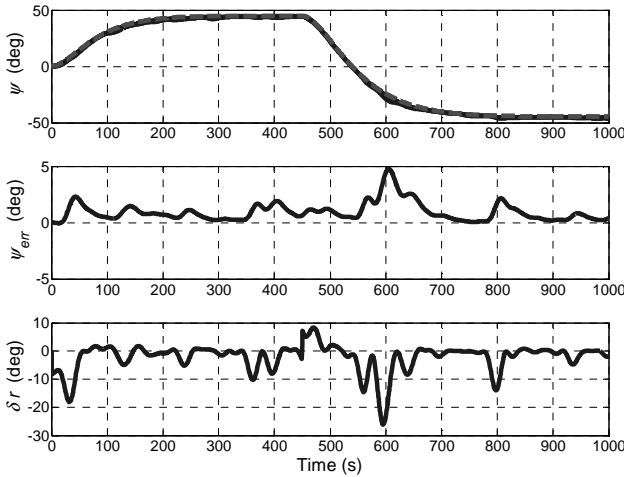


Fig 6. Cargo vessel with SM in the presence of wave disturbances.

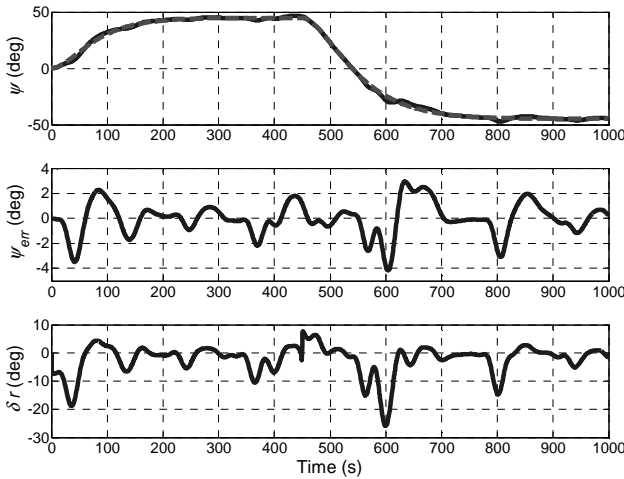


Fig 7. Cargo vessel with MPC in the presence of wave disturbances.

In the presence of wave disturbances (SM in Fig 6 and MPC in Fig 7), it can be noticed that the heading error for the cargo vessel with SM is $\pm 5^\circ$ and that with MPC is $\pm 4.2^\circ$. For wave is unmeasured disturbance (i.e. unpredictable), the main objective of the MPC is to minimise the tracking error. As a result, with the same wave disturbance, MPC is capable to minimise the heading error near to the zero margin. In terms of rudder deflection, both responses have very similar operational range. However, on close inspection, it can be noticed that the MPC is slightly smoother than that of SM.

In both cases for the cargo vessel, even with the presence of waves, both control methodologies are capable to deliver relatively accurate heading tracking with less than $\pm 4.2^\circ$ with a rudder operation range within $\pm 17^\circ$.

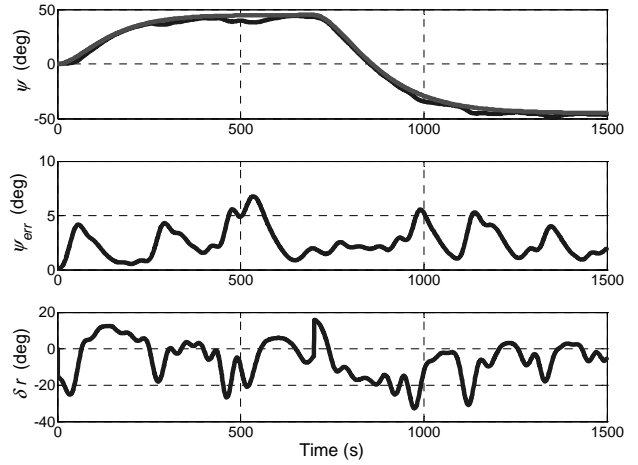


Fig 8. Oil Tanker with SM in the presence of wave disturbances.

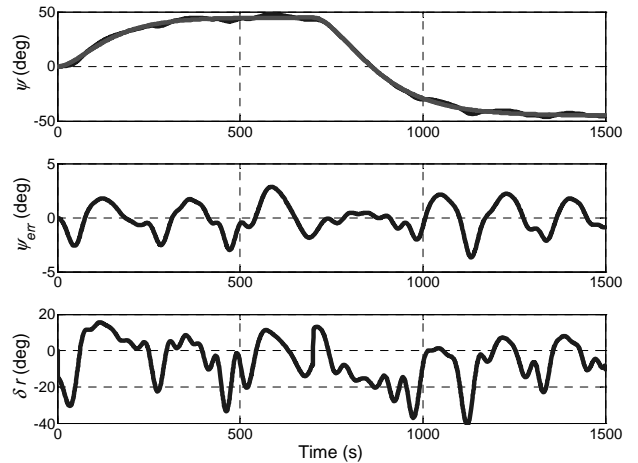


Fig 9. Oil Tanker with MPC in the presence of wave disturbances.

For the oil tanker application in the presence of waves (SM in Fig 8 and MPC in Fig 9), the heading error obtained for SM control is $\pm 6.8^\circ$, where as for MPC is $\pm 3.7^\circ$. The main advantage of MPC that can be noticed here is that the MPC is capable to minimise the heading error to around zero (the fluctuation along the zero margin). In addition, the rudder deflection patterns for both rudder deflection responses are very similar. However, MPC is able to predict ahead, as a result, even a slightly earlier rudder deflection will result in smoother process of minimising the heading error.

It can be noticed for the SM control theory, from Fig 6 and 8, the heading error response is almost a mirror image of the rudder deflection. This implies and confirms that sliding mode is behaving similarly to a high gain controller. On the other hand, MPC can minimise the heading error response more effectively with smoother rudder deflection response.

6. CONCLUSION

This paper has shown that with advanced optimal control methodology, MPC provides better overall performance in term of improved heading tracking ability by minimising the heading error. In addition, MPC is able to incorporate constraints into its controller; as it has taken into account the rudder constraints. As a result, it is able to deliver precise tracking without compromising the actuator operation (i.e. without driving the rudder deflection to its maximum). As a result, in terms of rudder manoeuvres, it has shown an outstanding accomplishment in term of safety, economy and general life span for the rudder actuator.

To summarise, the results from this investigation has indicated that MPC has improved the manoeuvring performance of the ships during course tracking compared with the performance of the Sliding Mode controllers. Consequently, if applied in practice, would offer the marine transportation a much safer process in the future.

REFERENCES

- Åström, K. J., & Källström, C. G. (1976). Identification of Ship Steering Dynamics. *Automatica*, **12**, 9-22.
- Bemporad, A., Morari, M., Dua, V. And Pistikopoulos, N.P. (2002), "The Explicit Linear Quadratic Regulator for Constrained Systems", *Automatica*, **28**, 3-20.
- Edwards, C. and Spurgeon, S. K. (1998). *Sliding Mode Control: Theory and Application*. London: Taylor and Francis.
- Fossen, T. I. (1994). *Guidance and Control of Ocean Vehicles*. John Wiley & Sons, Chichester.
- Healey, A.J. and Marco, D.B. (1992), "Slow Speed Flight Control of Autonomous Underwater Vehicles: Experimental Results with NPS AUV II", *Proc. of the Second International Offshore and Polar Engineering Conference*, San Francisco, 525-532.
- Källström, C.G., Åström, K.J., Thorell, N.E., Eriksson, J. and Sten, L. (1979). Adaptive Autopilots for Tankers. *Automatica*, **15**(3), 241-254.
- Loo, M., McGookin, E. W. and Murray-Smith, D. J. (2004), "Application of Inverse Model Control to IFAC Benchmark Models", *4th International Conference on Advanced Engineering Design (AED 2004)*, Glasgow, U.K.
- Loo, M. (2005), *Inverse Model Based Controller Design for Marine Vessel Applications: A Comparison Study Against Other Control Methodologies*. PhD Thesis, University of Glasgow, Glasgow, U.K.
- Maciejowski, J.M. (2002). *Predictive Control with Constraints*. Prentice Hall, Pearson Education Ltd, 2002.
- McGookin, E. W., Murray-Smith, D. J., Li, Y., & Fossen, T.I. (2000). The Optimisation of a Tanker Autopilot Control System Using Genetic Algorithms. *Transactions of the Institute of Measurement and Control*, **22**(2), 141-178.
- Skogestad S. and Postlethwaite, I. (1996) *Multivariable Feedback Control: Analysis and Design*, John Wiley & Sons, England.
- Tupper, E.C. (2004) *Introduction To Naval Architecture*, Elsevier Butterworth-Heinemann, 4th Ed., Oxford, U.K.

Appendix A. MODEL DEFINITIONS

The structure of the A and B matrix is given below with respect to Equation (1):

$$A = \begin{pmatrix} a_{11} & a_{12} & 0 \\ a_{21} & a_{22} & 0 \\ 0 & 1 & 0 \end{pmatrix}, B = \begin{pmatrix} b_1 \\ b_2 \\ 0 \end{pmatrix}$$

One cargo ship and one tanker are being investigated. Each of them is different from one another because of their unique A and B matrix, length and speed of vessel. With

reference to Equation (1), the values of each vessel are given below:

Table A.1: Data of each vessel in different classes.

	Cargo	Tanker
Length (m)	161	322
Breath (m)	23.2	49.83
Draft (m)	8.23	19.50
Speed (knot)	15	16
a_{11}	-0.770	-0.298
a_{12}	-0.335	-0.879
a_{21}	-3.394	-4.370
a_{22}	-1.627	-0.773
b_1	0.170	0.116
b_2	-1.627	-0.773

The speed values in Table A.1 are shown in knots. For simplicity, it is converted to metre per second (i.e. 1 m/s \approx 2 knot). In addition, the data given in Table A.1 is normalised such that the length unit is equal to length of ship, and the time unit is equal to time required for ship to travel a ship's length (Källström *et al.*, 1979). Because of these characteristics, the time scaling is used throughout the simulation has to be normalised accordingly in order to achieve the actual results (Källström *et al.*, 1979).